第39卷 第5期
2018年5月
焊 接 学 报
TRANSACTIONS OF THE CHINA WELDING INSTITUTION
Vol.39(5):059－062
May 2018

铝/铜异种金属熔钎焊接头微观组织与力学性能

周相龙， 石 玗， 朱 明， 顾玉芬
(兰州理工大学 省部共建有色金属先进加工与再利用国家重点试验室，兰州 730050)

摘 要：采用ER5356铝镁焊丝对1060纯铝与T2紫铜进行了脉冲旁路耦合电弧MIG熔钎焊，并对接头宏观形貌、微观组织及力学性能进行了分析．结果表明，在合适的焊接工艺参数下，可以获得成形美观、连续均匀、无缺陷的铝/铜异种金属接头．焊接接头从铜侧以金属间化合物层、Al-Cu共晶体向焊缝过渡，金属间化合物主要由脆硬的Al_2Cu相组成，而焊缝区主要由先析出的α(Al)固溶体以及从其晶界上析出的网状(Al)＋S(Al_2CuMg)/θ(Al_2Cu)共晶组织组成．随着焊接热输入的增加，金属间化合物层厚度明显增大，而焊接接头拉伸载荷先升高后下降，这与焊缝在铜母材上润湿铺展有关．接头拉伸时，主要在铝母材热影响区和焊缝与铜母材界面处发生断裂．

关键词：异种金属；脉冲旁路耦合电弧MIG熔钎焊；金属间化合物；拉伸载荷
中图分类号：TG 401　　文献标识码：A　　doi：10.12073/j.hjxb.2018390123

0 序 言

铜及其合金具有良好的导电、导热以及耐腐蚀性能，因此在电力、制冷以及化工等行业得到了广泛的应用．铜在国内作为稀缺资源，需从国外大量进口，价格高；而铝产能过剩十分严重，由于铝的导电和导热性能接近于铜，且有质轻价廉优势，以铝代铜，或是部分取代铜在“去产能”进程中将会有越来越广泛的应用前景[1－2]．然而铝、铜二者之间的固溶度低，熔点、线膨胀系数、热导率等物理性能存在显著差异，并且铝表面容易形成一层致密氧化膜，这使得铝/铜异种金属采用传统熔化焊方法难以实现可靠地连接[3]．而采用压力焊接和钎焊[4－5]方法，虽然可以获得质量性能都较好的接头，但这些方法设备复杂、成本高、效率低并且焊接尺寸受到限制．近年来，科技工作者对异种金属的连接进行了不断的探索，其中，采用熔钎焊方法有望解决这一问题，现已成为异种难焊金属连接领域的研究热点[6－7]．熔钎焊是利用异种金属熔点的差异，严格控制焊接热输入，使低熔点的铝熔化而高熔点的铜不熔化，借助熔化的铝在铜表面润湿铺展来实现铝－铜的连接．铝/铜熔钎焊时，通过降低焊接热输入，尽量减少铜基体的熔化，从而减弱两者的反应程度，减少界面金属间化合物层的厚度，提高接头的力学性能[8]．

文中采用新型高效低热输入的电弧焊焊接方法：脉冲旁路耦合电弧MIG焊(Pulsed DE-GMAW)[9]，该焊接方法能够在高熔敷率下有效地控制母材热输入．采用该方法对铝/铜异种金属进行搭接试验，并对接头微观组织和力学性能进行研究，为铝/铜连接的实际应用提供参考．

1 试验方法

试板尺寸为150 mm×50 mm×1 mm的1060纯铝和尺寸150 mm×50 mm×2 mm的T2紫铜．填充材料为直径1.2 mm的ER5356铝镁焊丝，焊丝的化学成分见表1．

表1 焊丝的化学成分(质量分数，%)

Table 1 Chemical composition of filterwire

Cu	Si	Mg	Fe	Zn	Mn	Al
0.05	0.25	5	0.5	0.05	0.15	余量

试验采用铝板在上、铜板在下的搭接形式，搭接宽度为10 mm，并将两者固定在焊接卡具上进行搭接焊，保证主路和旁路的焊枪在同一平面上，调整好焊枪之间角度(大约为45°)，并将焊丝尖端对准中间位置，其搭接方式如图1所示．焊前用钢丝刷对两种母材的表面进行打磨，除去氧化膜，用丙酮擦拭

收稿日期：2016－11－25
基金项目：国家自然科学基金资助项目(51675256)；省部共建有色金属先进加工与再利用国家重点实验室开放基金资助项目(SKLAB 020114208)；甘肃省基础研究创新群体计划项目资助项目(17JR5RA107)；甘肃省高效协同创新团队项目资助项目(2017C－07)

待焊区域,去除灰尘、油污. 采用氩气作为保护气,主路氩气流量为 20 L/min,旁路氩气流量为 5 L/min. 焊接工艺参数为:旁路、主路采用同步脉冲,脉冲频率 80 Hz,占空比为 15%,焊接速度 0.5 m/min,旁路电流固定为 25 A,主路电流在 45 ~ 65 A 范围内调节,即焊接电流为 70 ~ 90 A.

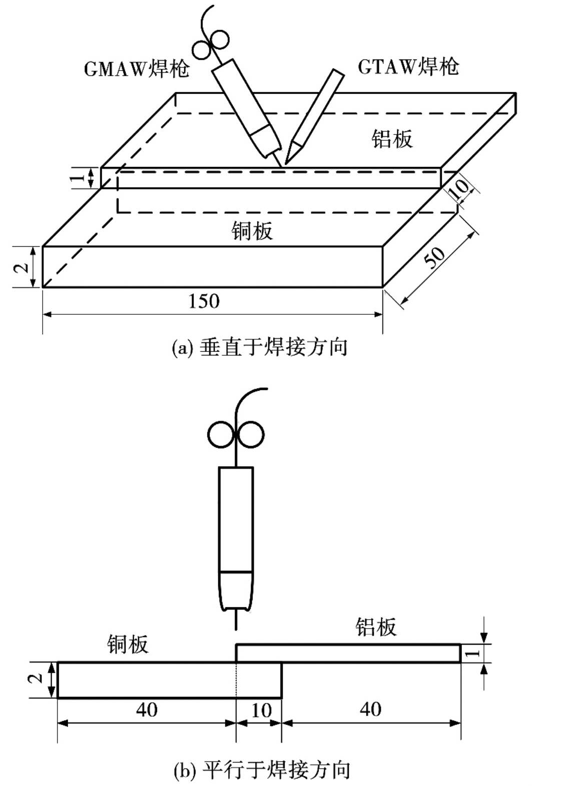

(a) 垂直于焊接方向

(b) 平行于焊接方向

图 1 铝/铜脉冲旁路耦合电弧 MIG 熔钎焊搭接示意图(mm)

Fig. 1 Schematic of Al/Cu Pulsed DE-GMAW lap welding-brazing

焊后对在不同焊接电流下得到的搭接接头进行打磨处理,并沿垂直于焊接方向截取试样进行标准金相试样制备. 采用带能谱的 JSM-5600LV 低真空扫描电子显微镜(SEM)对接头的微观组织和元素组成进行观察和分析,在 WDW-300J 型电子拉伸试验机进行力学性能试验,其加载速率为 1 mm/min,每组数据测试 3 次,然后取平均值,其拉伸试样的尺寸如图 2 所示.

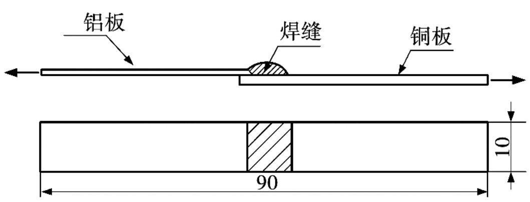

图 2 拉伸试样尺寸(mm)

Fig. 2 Dimension of tensile specimen

2 试验结果及分析

2.1 焊缝成形

图 3 为典型的铝/铜脉冲旁路耦合电弧 MIG 熔钎焊焊缝宏观形貌. 由图可知焊缝成形美观,连续均匀,无明显的裂纹、气孔等缺陷. 在焊接过程中,铝母材与填充焊丝熔化形成焊缝,而铜母材几乎未熔,由熔化的焊丝浸润铺展在其表面,形成了类钎焊接头. 整个焊接接头由铝熔合区、焊缝、界面过渡层组成.

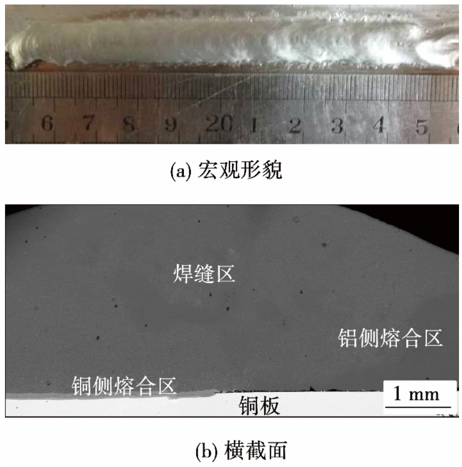

(a) 宏观形貌

(b) 横截面

图 3 铝/铜熔钎焊焊缝宏观及横截面形貌

Fig. 3 Weld appearance and cross-section of aluminum and copper

2.2 焊接接头微观组织分析

图 4 所示为不同焊接电流下铝/铜熔钎焊焊接接头界面过渡层的微观组织形貌. 由图可知,金属间化合物呈锯齿状向 Al-Cu 共晶区生长,并且随着焊接热输入的增加,不仅金属间化合物层厚度明显增大,而且 Al-Cu 共晶区厚度也明显增大. 当焊接热输入过大时,在金属间化合物层处产生细长的裂纹,这对接头力学性能会产生重要影响,如图 4c 所示.

为了进一步确定各区的组成,对图 4a 中 A 点、B 点、C 点和 D 点进行能谱分析,结果如表 2 所示. 由表可知,A 点靠近铜侧的金属间化合物层由 Al,Cu 两种元素组成,且 Al 的原子百分数为 67.3%,Cu 的原子百分数为 32.7%,Al,Cu 的原子比约为 2∶1,可以推断出该组织为 $\theta(Al_2Cu)$ 金属间化合物. B 点为 Al-Cu 共晶体组织,其中,Al 元素的原子分数为 81.4%,Cu 元素的原子分数为 16.9%,结合 Al-Cu 二元相图,可知该组织为 $\alpha(Al)+\theta(Al_2Cu)$ 共晶体组成. C 点为靠近 Al-Cu 共晶区亮灰色的焊缝组织,

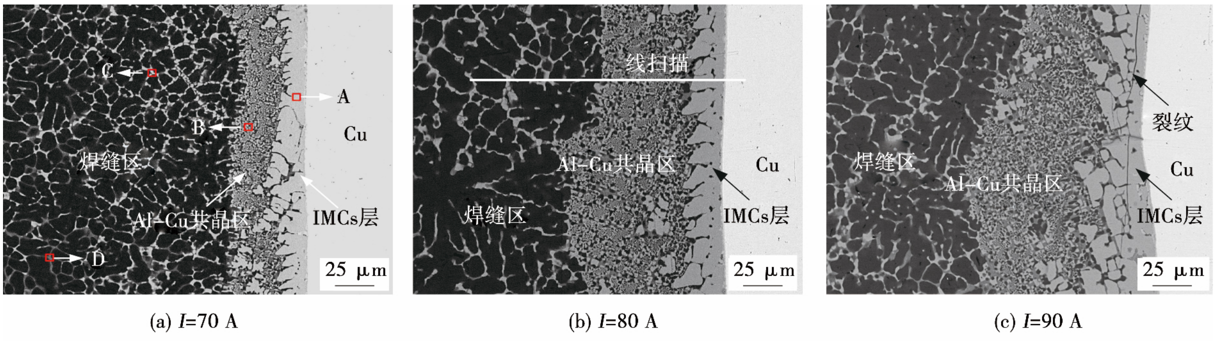

图 4　不同焊接电流下焊接接头微观组织

Fig. 4　Microstructures of weld joint at different welding currents

其中，Al 元素的原子分数为 72.3%，Cu 元素的原子分数为 26.4%，由此可知该组织仍由 α(Al) + θ(Al_2Cu) 组成. D 点为暗灰色的焊缝组织，其中，Al 元素的原子分数为 74.5%，Cu 元素的原子分数为 12.3%，Mg 元素的原子分数为 13.2%，结合相关文献[10]可推断出该组织为α(Al) + S(Al_2CuMg) 共晶体. 综上所述，焊缝区主要由先析出的 α(Al) 固溶体以及从晶界上析出的网状 α(Al) + S(Al_2CuMg)/θ(Al_2Cu) 共晶组织组成.

表 2　图 4a 所示位置 EDS 分析结果

Table 2　EDS analysis of positions shown in Fig. 4a

位置	原子分数 a(%)		
	Al	Cu	Mg
A	67.3	32.7	—
B	81.4	16.9	1.7
C	72.3	26.4	1.3
D	74.5	12.3	13.2

为了进一步分析铝/铜熔钎焊焊接接头界面过渡层的元素扩散情况，对图 4b 进行了线扫描，结果如图 5 所示.

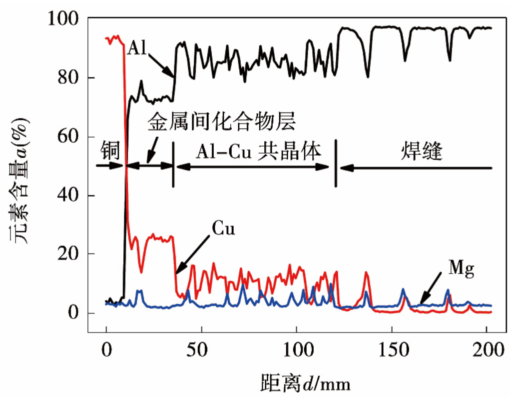

图 5　图 4b 线扫描分析图

Fig. 5　Linear scanning image of Fig. 4b

从铜侧到金属间化合物层，再到 Al-Cu 共晶区，最后到焊缝区，Cu 元素含量逐渐降低，而 Al 元素含量变化正好相反，并在金属间化合物层内 Al 与 Cu 元素含量相对稳定，出现明显的台阶，证实了此处有金属间化合物生成. 在 Al-Cu 共晶区 Al，Cu 元素含量起伏较大，说明该区中也有金属间化合物生成，并在基体中呈珊瑚状分布. 在焊缝区 Al，Mg，Cu 三种元素含量基本趋于平稳，波动处说明由 Al，Mg，Cu 三种元素组成的化合物生成.

2.3　接头强度

图 6 所示为不同焊接电流下所得接头拉伸试验结果，随焊接电流的增大，接头拉伸载荷先升高后下降. 当焊接电流为 80 A 时，接头具有相对较高的拉伸性能，拉伸载荷为 1 120 N. 此时熔化的焊丝及铝母材在铜母材上润湿铺展较好，冶金结合较为牢固，并且界面层的厚度较小，也未产生任何热裂纹(如图 4b 所示). 由此可知，焊缝与铜母材之间润湿铺展越好则接头力学性能相对越好，焊缝与铜母材之间界面层的厚度越小则接头力学性能相对越好. 因此，在脉冲旁路耦合电弧 MIG 熔钎焊过程中，通过

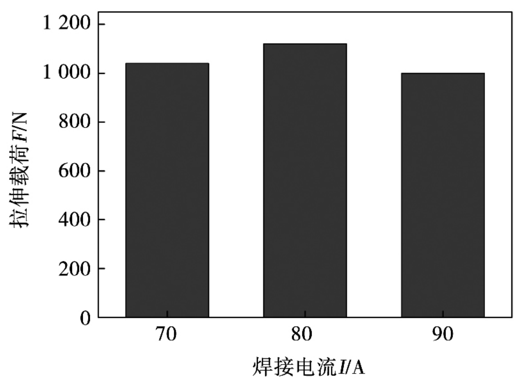

图 6　不同焊接电流下所得接头拉断载荷

Fig. 6　Tensile loads of joints obtained at different welding currents

控制焊接热输入,使得熔化的焊丝及铝母材在铜母材上润湿铺展良好,尽量减小接头界面层厚度,从而提高接头的力学性能.

2.4 断口形貌分析

图 7 所示为铝/铜异种金属焊接接头拉伸断口形貌. 通过拉伸试验研究表明,当接头力学性能较好时(如焊接电流为 80 A),试样经常在铝母材热影响区附近发生断裂,断口宏观表面有明显的颈缩现象,断口微观表面有较多细小的韧窝,如图 7a 所示,可判断为韧性断裂;当接头力学性能较差时(如焊接电流为 90 A),试样一般断裂于焊缝与铜母材界面处,可以看出断口表面整体较为平整,并分布着一些裂纹,如图 7b 所示,因此断口整体属于脆性断裂. 用 EDS 对图 7b 中断口表面的物相进行了分析,分析发现,整个接头断口表面主要由脆硬的 Al_2Cu 金属间化合物组成.

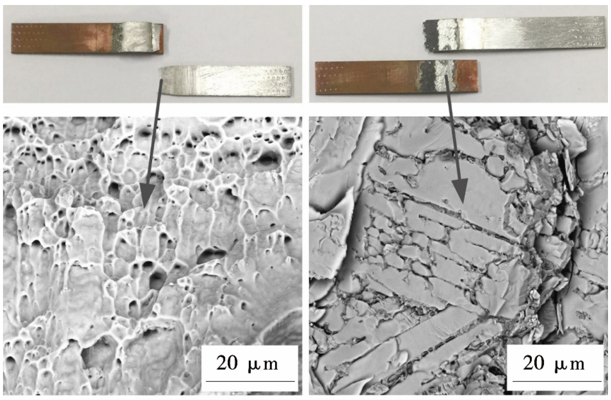

(a) 性能较好的断裂方式 (b) 性能较差的断裂方式

图 7 焊接接头拉伸断口形貌

Fig. 7 Fracture appearance of tensile specimens

3 结 论

(1) 采用脉冲旁路耦合电弧 MIG 熔钎焊方法,以 ER5356 为填充焊丝,可以获得成形美观、连续均匀、无缺陷的铝/铜异种金属接头.

(2) 铝/铜异种金属熔钎焊接头从铜侧以金属间化合物层、Al-Cu 共晶体向焊缝过渡,金属间化合物主要由脆硬的 Al_2Cu 相组成,而焊缝区主要由先析出的 α(Al) 固溶体以及从其晶界上析出的网状 α(Al) + S(Al_2CuMg)/θ(Al_2Cu) 共晶组织组成.

(3) 随着焊接热输入的增加,金属间化合物层厚度明显增大,而焊接接头拉伸载荷先升高后下降,最大拉伸载荷为 1 120 N,这与焊缝在铜母材上润湿铺展有关. 接头拉伸时,当接头力学性能较好时,试样经常在铝母材热影响区附近发生断裂,为韧性断裂形式;当接头力学性能较差时,试样一般断裂于焊缝与铜母材界面处,为脆性断裂形式.

参考文献:

[1] 张 满,薛松柏,姬 峰,等. $CuAl_2$ 相对铜铝钎焊接头组织与性能的影响[J]. 焊接学报,2011,32(2):93-96.
Zhang Man, Xue Songbai, Ji Feng, *et al*. Effect of $CuAl_2$ phase on properties and microstructure of Cu/Al brazed joint[J]. Transactions of the China Welding Institution, 2011, 32(2): 93-96.

[2] 夏春智,李亚江,王 娟. Cu/Al 异种金属连接的研究现状[J]. 焊接,2008(1):17-20.
Xia Chunzhi, Li Yajiang, Wang Juan. Research status of joining of Cu/Al dissimilar metals[J]. Welding & Joining, 2008(1): 17-20.

[3] 曲文卿,董 峰,齐志刚,等. 异种材料的连接[J]. 航天制造技术,2006(3):44-49.
Qu Wenqing, Dong Feng, Qi Zhigang, *et al*. Bounding of dissimilar metal materials[J]. Aerospace Manufacturing Technology, 2006(3): 44-49.

[4] Lee W B, Bang K S, Jung S B. Effects of intermetallic compound on the electrical and mechanical properties of friction welded Cu/Al bimetallic joints during annealing[J]. Journal of Alloys and Compounds, 2005, 390(1): 212-219.

[5] Ji Feng, Xue Songbai, Lou Jiyuan, *et al*. Microstructure and properties of Cu/Al joints brazed with Zn-Al filler metals[J]. Transactions of Nonferrous Metals Society of China, 2012, 22(2): 281-287.

[6] 彭 迟,程东海,陈益平,等. 铝/铜异种材料等离子弧熔钎焊搭接接头工艺分析[J]. 焊接学报,2016,37(4):65-68.
Peng Chi, Cheng Donghai, Chen Yiping, *et al*. Analysis process of plasama arc melting brazing lap joint of dissimilar materials of aluminum and copper[J]. Transactions of the China Welding Institution, 2016, 37(4): 65-68.

[7] 董 鹏,陈凯华,肖荣诗. 铝-铜异种金属激光深熔钎焊接头力学性能[J]. 中国激光,2011,38(6):129-133.
Dong Peng, Chen Kaihua, Xiao Rongshi. Mechanical properties of aluminum-copper joint by laser penetration brazing[J]. Chinese Journal of Lasers, 2011, 38(6): 129-133.

[8] 周 利,李志勇,赵洪运,等. 铝/黄铜异种金属 TIG 熔钎焊接头显微组织与力学性能[J]. 中国有色金属学报,2015,25(9):2389-2395.
Zhou Li, Li Zhiyong, Zhao Hongyun, *et al*. Microstructure and mechanical properties of Al/brass dissimilar metals TIG welding-brazing joint[J]. The Chinese Journal of Nonferrous Metals, 2015, 25(9): 2389-2395.

[9] 石 玗,温俊霞,黄健康,等. 基于旁路耦合电弧的铝钢 MIG 熔钎焊研究[J]. 机械工程学报,2011,47(16):25-29.
Shi Yu, Wen Junxia, Huang Jiankang, *et al*. Study on DE-GMAW MIG-brazing method for bonding steel with aluminum[J]. Journal of Mechanical Engineering, 2011, 47(16): 25-29.

[10] 蔡 华. 薄板 2524 高强铝合金光纤激光焊接接头组织及力学性能研究[D]. 北京:北京工业大学,2013.

作者简介: 周相龙,男,1990 年出生,硕士. 主要从事铝/铜异种金属连接工艺等方面的研究工作. 发表论文 4 篇. Email: zhouxiang0937@163.com

通讯作者: 石 玗,男,教授,博士研究生导师. Email: shiyu@lut.cn

following up with standard tensile and three-point bending experiments which were applied to obtain interface strength. In accordance with fracture toughness, a defection assessment was performed to provide the basis for enhancing welding joint strength. The results show that macro-segregation exists in the weld zone by using electron beam welding. According to interfacial strength characteristic of T2 copper/45 steel dissimilar materials, 2A level failure assessment based on BS7910 is applied and passed.

Key words: dissimilar material; weld appearance; welding joint strength; interface strength; defect assessment

Effect of magnetic field on the welding cladding morphology of thin walled parts LIU Haihua, ZHUO Yimin, LI Liangyu, YUE Jianfeng (Tianjin Key Laboratory of Modern Mechatronics Equipment Technology, Tianjin Polytechnic University, Tianjin 300387, China). pp 47 – 50

Abstract: For the problem of poor forming in the process of microbeam plasma welding caused by the downward flow of molten metal on both sides of thin-wall parts, the analysis of molten pool mechanical behavior and the research of pool forming control strategy are studied. The method of the external magnetic field is proposed for adding the inside of the electromagnetic pressure to the molten pool, intervening the downward flowing molten metal. The finite element software COMSOL is used to simulate the magnetic flux density, the induced current density and the electromagnetic force on the workpiece. Experiments of single-channel multi-layer welding are performed on 304 stainless steel, and the welding cladding morphology under different magnetic flux density was obtained. The results show that the magnetic field can significantly change the mechanical behavior and forming rules on the microbeam plasma welding, and can effectively restrain the flow of molten metal on the edge.

Key words: external magnetic field; thin-walled parts; cladding

Structure optimization design of CSP device based on Taguchi method XIONG Mingyue[1], ZHANG Liang[1,2], LIU Zhiquan[2], YANG Fan[1], ZHONG Sujuan[3], MA Jia[3], BAO Li[3] (1. School of Mechanical & Electrical Engineering, Jiangsu Normal University, Xuzhou 221116, China; 2. Institute of Metal Research, Chinese Academy of Sciences, Shenyang 110016, China; 3. State Key Laboratory of Advanced Brazing Filler Metals & Technology, Zhengzhou Research Institute of Mechanical Engineering, Zhengzhou 450001, China). pp 51 – 54

Abstract: In order to improve the solder joint reliability of chip scale package (CSP) devices, based on the Taguchi method, the stress-strain distributions of the CSP device under thermal cycling are simulated by using the steady-state constitutive equations of Garofalo-Arrhenius and the finite element method. Considering the solder joint material, solder joint height, chip thickness and the thickness of the substrate four factors, using Taguchi method and orthogonal table $L_9(3^4)$ to arrange the experiment, the study found that the main influencing factors of solder joint reliability are the solder joint material and the height of solder joints. Optimized by Taguchi method, the best combination of materials is solder material Sn3.9Ag0.6Cu, solder joint height 0.29 mm, chip thickness 0.1 mm and substrate thickness 0.17 mm. Compared with the original design scheme, the optimal scheme reduces the creep strain energy density by 65.4% and the signal-to-noise ratio by 9.22 dB. The results show that the reliability of CSP solder joints is significantly improved.

Key words: chip scale package; Taguchi method; thermal cycling; solder joint

Dissimilar friction stir welding of Al/Mg alloys based on non-rotational shoulder LI Feng[1], DANG Pengfei[1], Liu Xuesong[2] (1. CSR Qingdao Sifang Co., Ltd., Qingdao 266111, China; 2. State Key Laboratory of Advanced Welding and Joining, Harbin Institute of Technology, Harbin 150001, China). pp 55 – 58

Abstract: Welding tool is the core of FSW, which plays a significant role on joint quality. In this paper, a non-rotational tool system was employed to join 6061-T6 and AZ31B alloys. Joint formation and mechanical property of joints based on traditional and non-rotational shoulder processes were mainly analyzed. The results showed that compared with traditional tool, the smooth surface appearance was attained and complex Al/Mg intercalated layer structures and bended Al/Mg joining interface formed in nugget zone based on non-rotational shoulder tool system, improving mechanical interlocking effectively. Moreover, the thickness of intermetallic compounds layer was also smaller than those of traditional tool, resulting from the severer stirring actions and heat sink induced by the non-rotational shoulder. The maximum tensile strength of joint obtained by non-rotational shoulder reached 137 MPa, which was improved by 28% compared with traditional tool.

Key words: friction stir welding; non-rotational shoulder; dissimilar Al/Mg alloys; microstructure; tensile strength.

Microstructure and mechanical properties of Al/Cu dissimilar metals welding-brazing joint ZHOU Xianglong, SHI Yu, ZHU Ming, GU Yufen (State Key Laboratory of Advanced Processing and Recycling of Nonferrous Metals, Lanzhou University of Technology, Lanzhou 730050, China). pp 59 – 62

Abstract: Dissimilar metals of 1060 aluminum and T_2 copper were joined with lap joint by pulsed double electrode gas metal arc welding-brazing with ER5356 $AlMg_5$ filler wire. Microstructure, elements composition and mechanical properties of joint were studied. The results showed that good-looking, continuous and uniform, defectless welds could be obtained with proper welding parameters. Welded joints transit from copper side with intermetallic compound (IMC) layer, Al-Cu eutectic to welding seam. The IMC layer is composed of Al_2Cu phase, and the weld zone is composed of α(Al) solid solutions and α(Al) + S (Al_2CuMg)/θ(Al_2Cu) eutectic in the grain boundary. The thickness of IMC layers increases with the increase of welding heat input, while the tensile load of joint increases at first and then decreases, which is related to the wetting and spreading of the weld on the copper base material. Tensile test results show that the joint fractures at the heat affected zone of aluminum base metal or interface layer between the weld and the copper base metal.

Key words: dissimilar metals; pulsed DE-GMAW welding-brazing; intermetallic compounds; tensile load

Microstructure and mechanical properties of fiber laser welding of 950 MPa grade twinning-induced plasticity steel for automotive industry HAN Zhiqiang[1], DONG Danyang[2], LIU Yang[1], JIN Sen[2], TANG Zhenyu[2] (1. School of Materials Science and Engineering, Northeastern University, Shenyang 110819, China; 2. College of Science, Northeastern University, Shenyang 110819, China). pp 63 – 68